Orientation Anisotropy of the Mechanical α Relaxation of High-Density Polyethylene Films Having a Well-Defined Stacked Lamellar Morphology

Hongyi Zhou and Garth L. Wilkes*

Polymer Materials and Interfaces Laboratory, Chemical Engineering Department, Virginia Polytechnic Institute and State University, Blacksburg, Virginia 24061

Received September 26, 1996; Revised Manuscript Received February 4, 1997

ABSTRACT: Dynamic mechanical experiments were conducted on melt-extruded uniaxially oriented high-density polyethylene films having a well-defined stacked lamellar morphology. Samples were cut at different angles with respect to the original machine direction (MD) and tested by increasing the temperature from 20 to 130 °C at a heating rate of 0.5 °C/min in the frequency range from 0.01 to 10 Hz. Samples before and after the dynamic mechanical tests were also investigated by using WAXS, SAXS, and DSC. Oscillating parallel (0°) and perpendicular (90°) to the MD gave rise to a single tan δ dispersion peak, while oscillating at angles between the above two extremes generated a secondary dispersion peak at lower temperatures, with a maximum relaxation strength occurring at 45° orientation. It was concluded that, for the 0 and 90° orientations, the mechanical dispersion arises essentially from the crystalline phase, and it contains the contributions of earlier recognized intralamellar (α_I) and intracrystalline (α_{II}) relaxations. For the 45° orientation, the mechanical dispersion is believed to originate from an activated interlamellar shear motion that is related to the characteristics of the interface between the crystalline lamellar phase and the amorphous phase.

Introduction

Under dynamic small-strain studies, polyethylene (PE) displays at least three mechanical relaxations, designated as α, β, and γ in order of decreasing temperature, in addition to the melting point.[1] The γ relaxation, displayed by bulk-crystallized linear and branched PE and solution-grown PE single-crystal mats, is found in the temperature range of −150 °C to −120 °C. The β relaxation, distinctly displayed only by bulk-crystallized branched PE, is in the temperature range of −30 to +10 °C. The α relaxation, shown by bulk-crystallized linear and branched PE and solution-grown PE single-crystal mats, is in the temperature range of 30 to 120 °C.[1−3] As expected, all peak positions increase with frequency, and each may be influenced by thermal history.

The origins of the three mechanical relaxations have been *extensively studied* in the past.[2−22] Although some detailed molecular assignments are still open to debate, the reality of the basic relaxation processes is clear; these have been well summarized by Boyd.[2,3] The α and β relaxations are commonly attributed to the relaxation mechanisms in the crystalline phase and amorphous phase, respectively; the γ relaxation is, according to different authors, due to the localized motions of either chain ends or branches associated with the amorphous phase[1,5] although originally, it was proposed to arise also from the crystalline phase.[6] Complementary dielectric relaxation studies on the respective α, β, and γ relaxations in PE have also been carried out and are well summarized.[23]

The mechanical α relaxation for HDPE covers a wide temperature range from 30 to 120 °C, and the calculated activation energy is a somewhat "diffuse" value, ranging from 90 kJ/mol to more than 300 kJ/mol.[1−3] In addition, the mechanical dispersion, as measured by tan δ, is not symmetric, as exemplified by the data in Figure 1 that were obtained for a compression-molded, slow-cooled unoriented HDPE film utilizing the same resin that was used to produce the uniaxially oriented HDPE films that will be the focus of this report. All these facts have led to the assumption that the major mechanical α relaxation consists of several subrelaxations, and this is known as the multiplicity of the mechanical α relaxation for HDPE. At least three subrelaxations, namely α_I, α_{II}, and α_{III} in order of increasing temperature, have been proposed.[7−22]

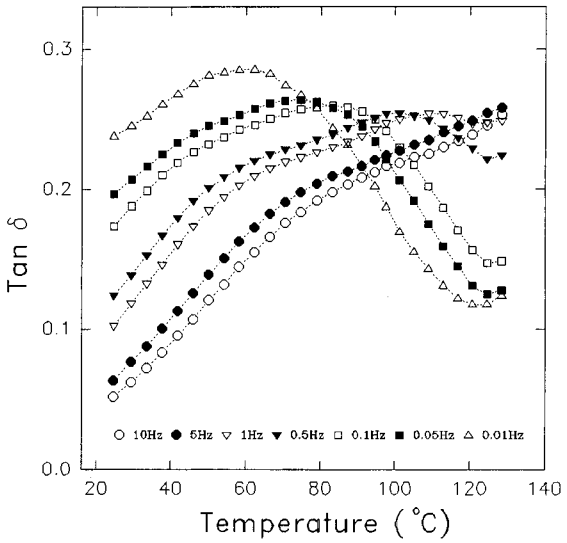

Figure 1. Typical tan δ plot for unoriented HDPE materials.

The resolution of the mechanical α relaxation into two components was first reported by Nakayasu et al.[7] The subrelaxations were designated as mechanism I (later α_I) at lower temperatures and mechanism II (later α_{II}) at higher temperatures, and they were stated to display activation energies of 117 and 210 kJ/mol, respectively. The authors suggested that the α_I process was associated with intercrystalline (grain boundary) relaxation phenomena, and the α_{II} process was related to intracrystalline (single chain) relaxation phenomena. The

* To whom correspondence should be addressed.
⊗ Abstract published in *Advance ACS Abstracts,* April, 1; 1997.

S0024-9297(96)01437-4 CCC: $14.00

existence of a third subrelaxation at even higher temperature was also speculated, but no molecular assignment and activation energy were provided by the authors.

By comparing the dynamic mechanical test data for melt-crystallized HDPE films, which showed two relaxation peaks (α_I and α_{II}), with that of PE single-crystal mats, which showed only one relaxation peak (α_{II}), Takayanagi et al. concluded that the α_I mechanism was complicated thermorheologically; however, the α_{II} mechanism was viewed as a thermorheologically simple process.[8−10] Their justifications were based on the construction of the master curves (based on the loss modulus E'') for both relaxations. The construction of master curves for the α_{II} relaxation needed only horizontal shifts, whereas for the α_I relaxation, both horizontal shifts and vertical shifts were needed. By plotting horizontal shift factors versus reciprocal temperature, the activation energies for the α_I and α_{II} relaxations were found to be 125 and 192 kJ/mol, respectively—these values being close to those expressed above. The authors suggested that the deformation of intermosaic regions within the crystalline lamellae was the origin of the α_I relaxation, and the α_{II} relaxation arose from the rotational oscillation of polymer chains in the crystal lattice.

Dynamic mechanical tests (parallel to the orientation axis), dynamic X-ray scattering experiments, and NMR experiments for oriented PE films have been carried out by McCrum et al.,[11,12] Stein et al.[13,14] and Ward et al.[15,16] These authors concluded that interlamellar shear, or interlamellar slip, was the origin of the α_I relaxation, and it was sensitive to the morphology of the specimens used. The α_{II} relaxation was believed to originate from the viscous nature of polymer chain motions in the crystal lattice at high temperatures, including twisting motion about the *c*-axis as well as transitional motion along the *c*-axis.

Since most of the studies dealing with the mechanical α relaxation were performed on HDPE having spherulitic morphology or initially spherulitic texture prior to deformation, it has therefore been difficult to give unambiguous interpretations of the relaxation mechanisms because of the structural complexities of the spherulites or remnants of that texture. Depending on the local orientation of the lamellae and associated interlamellar amorphous layers, all types of inter- and intralamellar motions might be expected to take place in the specimen during the dynamic mechanical test at the appropriate frequency and temperature. Therefore, it is desirable to utilize materials having a more simplified and well-defined morphology to carry out dynamic mechanical experiments, with the hope that such morphologies may assist in better defining the nature and origin of a given mechanical relaxation.

Matsuo et al.,[17] Ogita et al.,[18] and Ohta et al.[19] also carried out dynamic mechanical experiments and creep experiments for ultrahigh molecular weight polyethylene (UHMwPE) that had been ultradrawn into fibers. These authors showed the existence of the third relaxation (α_{III}), in addition to the α_I and α_{II} relaxations. It was suggested that the α_{III} relaxation was related to the transition from the orthorhombic phase to the hexagonal-packed phase at high temperatures. Furthermore, by using fibers at different draw ratios (orientation states), it was shown that the strength of the α_{II} relaxation (along the fiber axis) became smaller with increasing draw ratio and finally reached zero at a draw ratio of 400. In addition, the calculated activation energy of the α_{II} relaxation changed with the orientation state of the fibers. Therefore, the strength of the α_{II} relaxation was suggested to be related to the anisotropy of the crystal lattice potential. The α_I mechanism, however, was suggested to be related to an intralamellar grain boundary phenomenon that was associated with a rotational motion of crystal grains in the direction of external excitation.

Since most of the dynamic mechanical tests were done by isochronal scans at specific heating rates, it has been suspected that the morphology of the specimen might have been changed during the experiments; therefore, it is desirable to carry out the tests isothermally. By doing isothermal dynamic mechanical tests for HDPE and lightly cross-linked low-density polyethylene over a wide region of frequency (10^{-4} to 1 Hz), Amparo et al. concluded that the multiplicity of the mechanical α relaxation was due to the size (thickness) distribution of the crystalline lamellae.[20−22] In other words, these researchers proposed that the α_I and α_{II} relaxations originate from the same molecular mechanism (defect motions in crystalline lamellae) within thinner and thicker crystalline lamellae, respectively. The confusion about the multiplicity of the mechanical α relaxation, according to the authors, was mainly due to the fact that the lamellar thickness distribution was probably changed at high temperatures during the isochronal dynamic mechanical measurements.

A review of the literature on the mechanical α relaxation for HDPE has shown that the longstanding controversy has not been resolved. Two principal reasons are (1) the complex morphologies of the specimens and (2) the speculated morphological changes during the dynamic mechanical tests. More specifically addressing the former, in the case of a spherulitic morphology, the inter- and intralamellar motions can always happen simultaneously during the dynamic tests, and this could result in the concurrence of both the α_I and α_{II} relaxations. For the fibril morphology possessed by the UHMwPE ultradrawn fibers, the existence of the chain-extended crystalline phase and the orientation state of the ordered amorphous phase must certainly have some influence on the mechanical α relaxation. In addition, the morphologies of the samples before and after dynamic mechanical tests are not to be expected to be exactly the same due to lamellar thickening etc.; thus, it should be further investigated to assure the effects of such morphological changes on the mechanical α relaxation.

In the study presented here, melt-extruded uniaxially oriented HDPE films were used, and mechanical oscillations were applied at different orientations with respect to the original machine direction (MD). In contrast, for the case of UHMwPE ultradrawn fibers, the original MD is the only possible oscillation direction. Oscillation in different directions may excite specific relaxation processes due to the different molecular motions generated, and this in principle may make it easier to understand the separate relaxation processes. Isochronal tests were carried out in this study, since they have the advantage of covering a large range of temperature. In this case, morphological features for the specimens before and after dynamic mechanical tests were also investigated.

As a result, the orientation anisotropy of any mechanical dispersion itself is an important issue for many polymers that are used at an oriented state (such as

packing films etc.) in engineering applications. For example, the damping character of a material, which is closely coupled to the dynamic mechanical dispersion, may be more or less activated at different orientations with respect to the loading direction and therefore influence the character of the energy dissipation ability of the material. Therefore, it is also the purpose of this study to provide dynamic mechanical test data that reflect information on this issue as well.

Experimental Section

Materials. The linear HDPE homopolymer resin studied had a number-average molecular weight and a weight-average molecular weight of 14 600 and 150 000, respectively. The 1 mil thick melt-extruded films were kindly provided by Hoechst Celanese Co. Under the film extrusion processing conditions, the crystalline phase became quite highly uniaxially oriented with the *c*-axis along the MD. This was quantified by determination of the Hermans' orientation function, f_c, for the crystalline phase using X-ray scattering, where f_c is defined as

$$f_c = \frac{1}{2}(3\langle\cos^2\theta\rangle - 1) \quad (1)$$

In eq 1, the quantity $\langle\cos^2\theta\rangle$ represents the average value of $\cos^2\theta$, with θ being the angle between the *c*-axis in the crystal (chain axis direction) and the MD axis. The amorphous phase, however, had no significant orientation as determined from a previous study.[24] In the present study, both melt-extruded film (precursor film) and annealed precursor films were used. Two different kinds of annealed films were used. One was provided by Hoechst Celanese Co., where annealing was done by passing the precursor films through an oven at 120 °C with a certain on-line speed that allowed the materials to remain at this temperature for ca. 20 min. Since there was a small amount of tension (ca. 3% strain) associated with this process, this kind of annealed film will be referred to as a tension-annealed film. In addition, free-annealed films, produced simply by annealing the precursor films without tension at 120 °C for 20 min, were also used.

Dynamic Mechanical Analysis. Samples (5 cm wide and 10 cm long) for dynamic mechanical tests were carefully cut directly from the HDPE films at different angles with respect to the original MD, with 0° being parallel and 90° perpendicular to the MD. The dynamic mechanical parameters of storage modulus (E'), loss modulus (E''), and loss factor ($\tan\delta$) were determined using a Seiko DMS instrument (Model 210). Temperature was increased from 20 to 130 °C at a heating rate of 0.5 °C/min. Frequencies covered a wide range from 0.01 to 10 Hz. During the experiments, the applied tensile force was kept small to ensure a linear viscoelastic response from the specimen.

WAXS and SAXS. All the WAXS experiments were performed by utilizing a Philips tabletop X-ray generator (Model PW1720) equipped with a standard vacuum-sealed Warhus photographic pinhole camera. The instrument with Cu Kα radiation (λ = 1.54 Å) was operated at 40 kV and 20 mA. Single-layer film and stacks of films were used as the specimens for the experiments. A Kratky slit-collimated camera was used for the SAXS experiments. In this case, the scattered intensity was monitored by a one-dimensional position-sensitive detector, corrected for sample thickness, counting time, and transmission, and standardized to a Lupolen-based standard. In all the SAXS experiments, the specimen's MD was aligned parallel to the width's direction of the sample holder so that X-ray scans were along the MD (MD scans).

Differential Scanning Calorimetry. DSC experiments were carried out by using a Seiko DSC instrument (Model 220C). A heating rate of 10 °C/min was used. In all the experiments, the samples' weight was kept essentially constant (ca. 5 mg). An estimate of lamellar thickness and its distribution were obtained by applying the Gibbs−Thomson equation to the DSC data,[25] and the heat flow versus temperature curves were transformed into plots of relative probability versus lamellar thickness by using the same equation as proposed by the authors of ref 19. In the calculations, the heat of fusion of the crystal phase and the free energy of the basal surface of the crystalline lamellae used were 290×10^6 J/m^3 and 90×10^{-3} J/m^2, and the equilibrium melting temperature was chosen as 145.5 °C.[26] [A detailed study on the applicability of DSC to determine the crystalline lamellar thickness and its distribution has recently been carried out by the same authors of this report and submitted for publication.[27]]

Transmission Electron Microscopy. Samples for the TEM study were treated by chlorosulfonic acid at 60 °C for 6 h; then they were washed with sulfuric acid and water and dried overnight. The stained samples were embedded in an epoxy resin and cured at 65 °C overnight. The embedded samples were microtomed at room temperature by cutting along the MD. The microtomed thin sections of ca. 80 nm thick were used for the TEM observations after being treated by uranyl acetate. All the TEM work was performed by using a Philips EM420 instrument operated at 100 kV.

Results

Figure 2 shows the WAXS patterns for the tension-annealed film used in this study. It is obvious from these patterns that the crystalline phase is quite well oriented with the *c*-axis along the MD (Figure 2b,c). In addition, the patterns also illustrate that the *a*- and *b*-axes are principally uniformly distributed in the plane perpendicular to the MD (Figure 2a), which contains the transverse direction (TD) and the normal direction (ND) of the film. The Hermans' orientation functions for the crystalline phase (f_c), calculated from the WAXS patterns, are 0.67, 0.80, and 0.68 for the precursor film, tension-annealed film, and free-annealed film, respectively. The TEM micrograph shown in Figure 3 presents a direct visualization of the well-defined stacked lamellar morphology possessed by the same films whose WAXS patterns were shown in Figure 2. TEM experiments for the precursor film and the free-annealed film revealed the same kind of well-defined stacked lamellar morphology, except that for the precursor film, the crystalline lamellae were somewhat thinner and displayed less contrast than those of the annealed films. No distinct difference was observed between tension- and free-annealed films by TEM.

Anisotropy of the Mechanical α Relaxation. The relaxation behavior for the precursor film determined at different orientations with respect to the MD is presented in Figure 4. These data clearly show the anisotropy (orientation dependence) of the mechanical α relaxation. For the 0° oscillation (dynamic mechanical test parallel to the MD), only one single dispersion peak was observed, at approximately 84 °C at 0.1 Hz. The 90° oscillation (dynamic mechanical test perpendicular to the MD) also showed only one dispersion peak, but this time the peak occurred at ca. 96 °C at the same frequency—a distinctly higher temperature than that of the 0° oscillation. For all the other orientations investigated, a secondary dispersion peak at low temperatures was found. The existence of the secondary peak was confirmed by duplicating the experiment for the same type of sample to make sure that it was not coming from experimental errors. The strength of the secondary dispersion peak was dependent on the sample orientation in the DMTA experiment, with a maximum in dispersion strength occurring at ca. 45° orientation. However, the temperature of the secondary dispersion peak remained essentially unchanged with sample orientation. It is worth noticing that, although the intensity of the major peak and that of the secondary

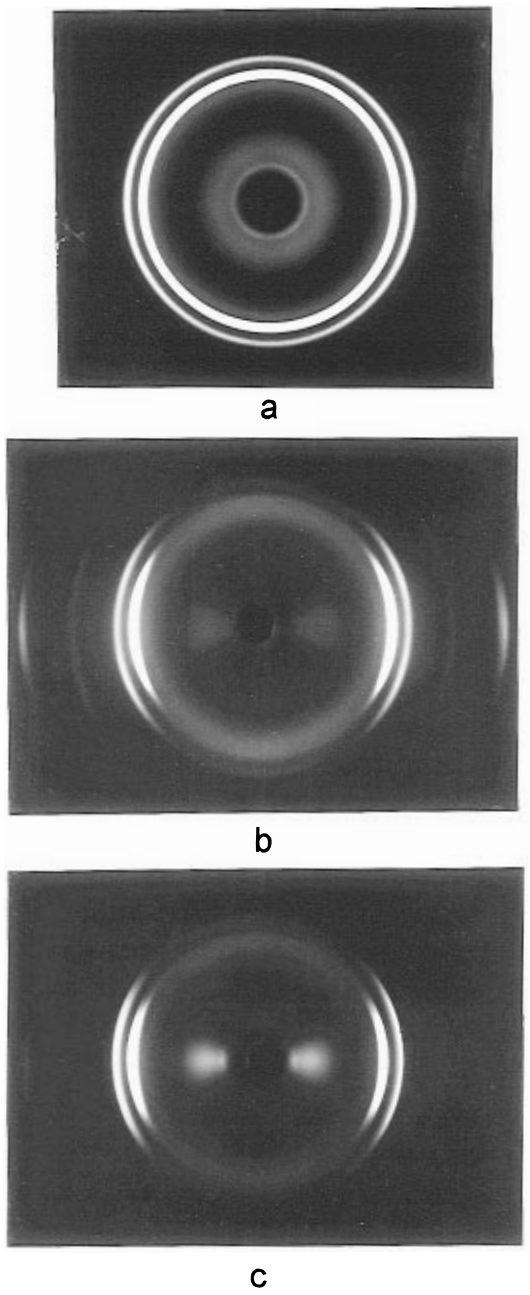

Figure 2. WAXS patterns for the tension-annealed film with the X-ray beam parallel to (a) the MD, (b) the ND, and (c) the TD.

peak varied with sample orientation, total dispersion (the area under the whole tan δ curve) remained basically constant for all sample orientations when compared in the temperature range investigated.

The results of tan δ at the frequency of 0.1 Hz for all the orientations are shown in Figure 5, where tan δ is plotted against temperature and orientation. Again, the orientation dependence of the mechanical α relaxation is clearly shown. We now address some features of the relaxation peaks in Figure 5, the first being the calculation of the respective activation energies. In order to do so, master curves were constructed. From the Arrhenius-type plot of horizontal shift factors versus reciprocal temperatures utilized in constructing these plots, the activation energies were obtained. Mechanical loss modulus (E'') was used in the construction of the master curves since it is a single variable as compared to the mechanical dispersion tan δ, which is

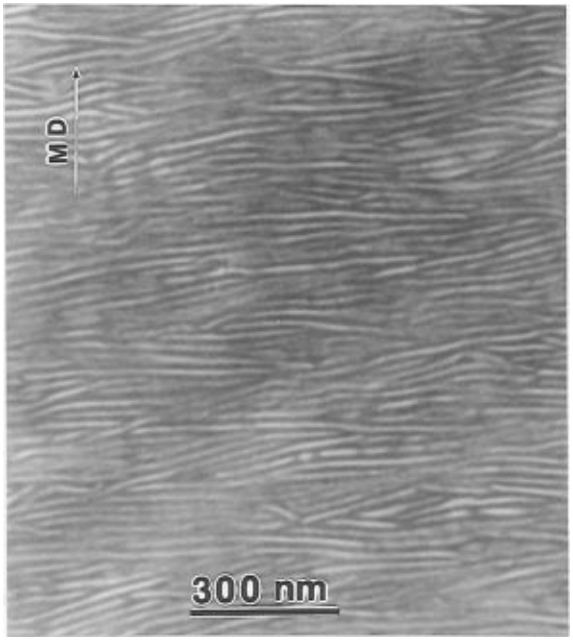

Figure 3. TEM micrograph showing the stacked lamellar morphology for the tension-annealed film. MD represents the machine direction.

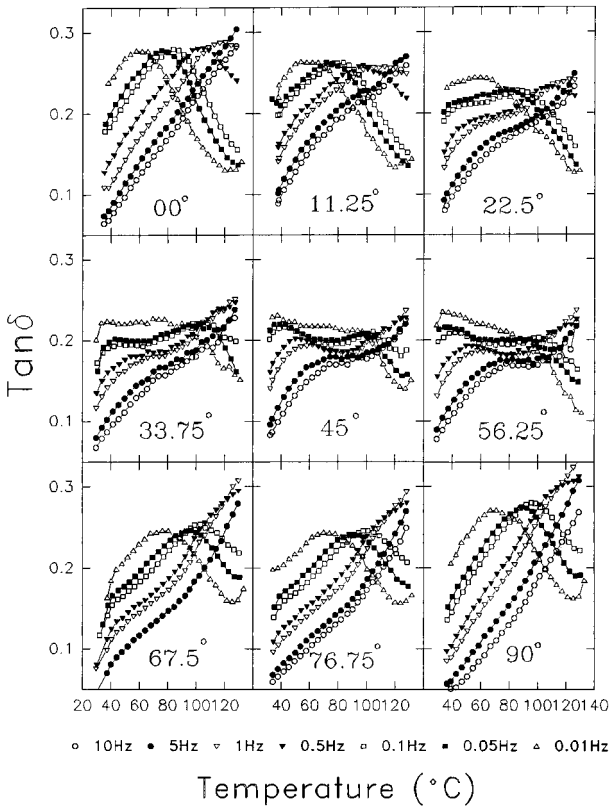

Figure 4. Mechanical relaxation for the precursor film at different orientations (angle shown on each plot) with respect to the original MD.

dependent upon both the storage modulus (E') and the loss modulus (E'').

The loss moduli for the 0, 45, and 90° oscillations are shown in Figure 6. For each orientation, a master curve based on the loss modulus was constructed by shifting each individual curve to the reference temperatures horizontally and then vertically to obtain the best superposition. The master curves thus obtained are shown in Figure 7. It can be seen that the superposition

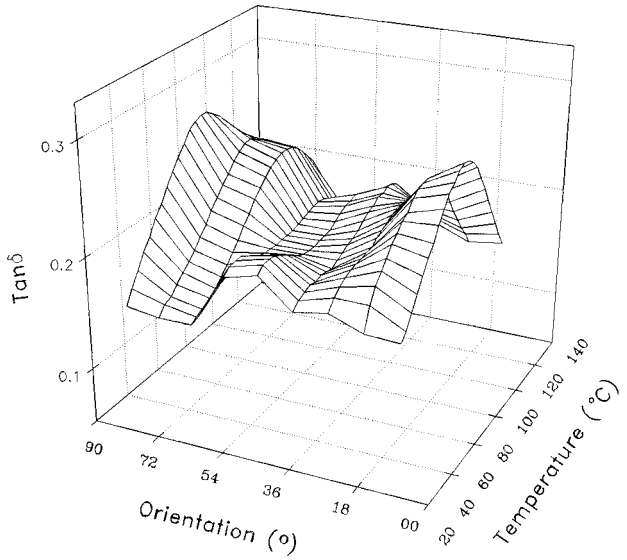

Figure 5. Tan δ surface plot for the precursor film showing the orientation dependence of the mechanical α relaxation.

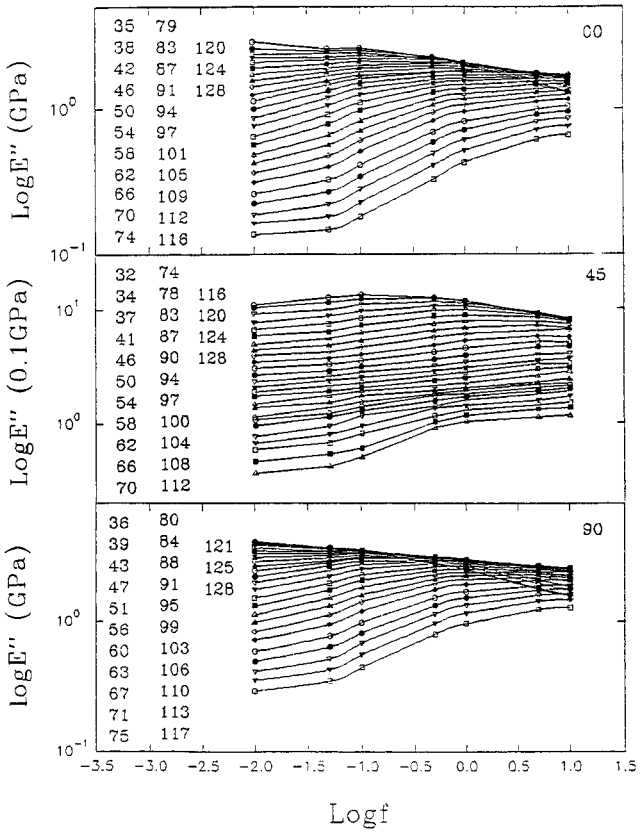

Figure 6. Dynamic mechanical loss modulus for the precursor film at the 0, 45, and 90° orientations.

was quite good, except at lower frequencies; this is especially true for the case of the 45° oscillation. It is noticed that these master curves are somewhat diffuse, which is very representative of its expected behavior based on past studies of high-density polyethylene.[16−18] However, the orientation dependence behavior is still obvious; i.e., those for the 0 and 90° oscillations had a broader and *flatter* peak while that for the 45° oscillation showed a broad dispersion with the existence of *two subpeaks*.

Figure 8 represents the corresponding horizontal shift factors and vertical shift factors for the construction of the master curves at the three orientations. The

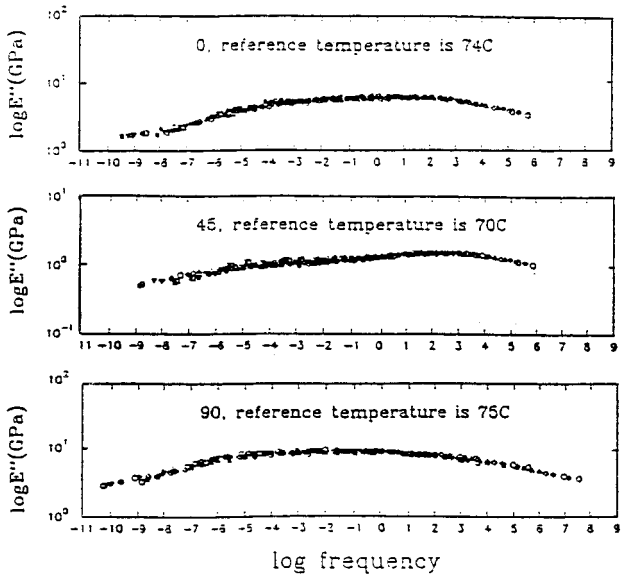

Figure 7. Master curves based on the dynamic mechanical loss modulus for the precursor film at the 0, 45, and 90° orientations.

horizontal shift factors were plotted against reciprocal temperature to calculate activation energy, and the vertical shift factors were plotted against temperature to take into account the change of modulus with respect to temperature. It is evident that the vertical shifts became larger at temperatures *higher than* 110 °C, and this suggests that the time−temperature superposition is not valid and therefore consistent with the poor superposition of the master curves shown in Figure 7. Therefore, all the data used in the calculation of the activation energy were at temperatures below 110 °C. The slopes of the linear regions on these plots were obtained by using linear regression when the R values were larger than 0.99. The calculated activation energies are shown on the Arrhenius plot at each orientation.

Effect of Conditions of Thermal Annealing on Tan δ. The tan δ plot similar to that of Figure 5 for the tension-annealed film is presented in Figure 9. Once again, at the 0 and 90° orientations, tan δ showed only one overall relaxation peak, with the 0° orientation displaying the peak at a lower temperature than that of the 90° oriented sample at the same frequency. A secondary relaxation peak existed at all other orientations, with a maximum occurring at the 45° orientation. For a given orientation, other noticeable features as compared to Figure 4 are (1) the strength of the primary dispersion was decreased and (2) the primary relaxation peaks became broader.

In Figure 10, tan δ (at 0.1 Hz) has been plotted against temperature for the melt-extruded film (pre), tension-annealed film (T120), and free-annealed film (F120) at the three orientations of 0, 45, and 90°. In addition to the above-mentioned differences in tan δ, the effects of tension in the annealing process deserve particular attention. For the free-annealed samples, the major change observed relative to the behavior of the precursor sample was a decrease in dispersion strength; for the tension-annealed samples, a distinct shifting of the dispersion peak to higher temperatures occurred, in addition to a decreased dispersion intensity, especially noted for the 0° orientation. For the case of the 45° orientation, the low-temperature relaxation remained basically intact, with all data overlapping for

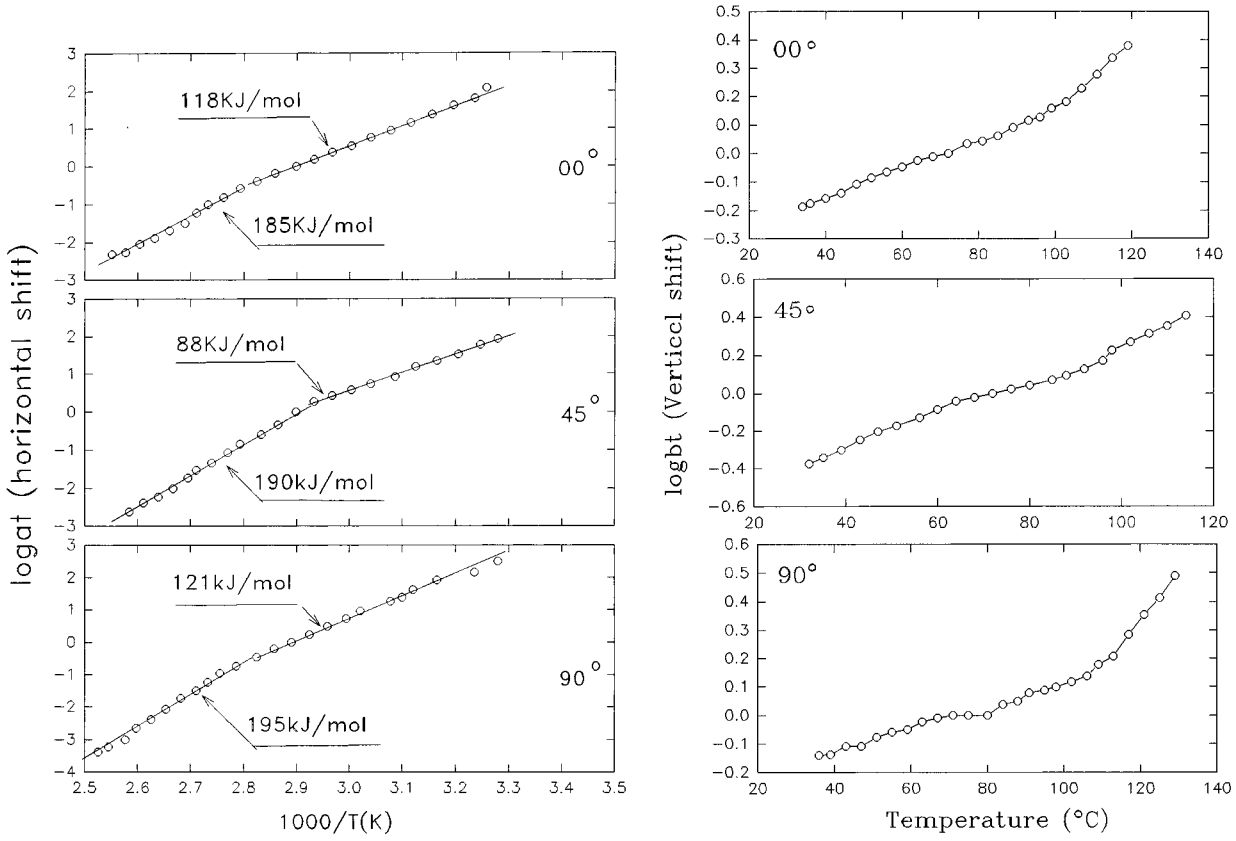

Figure 8. Horizontal and vertical shift factors for the construction of master curves for the precursor film at the 0, 45, and 90° orientations.

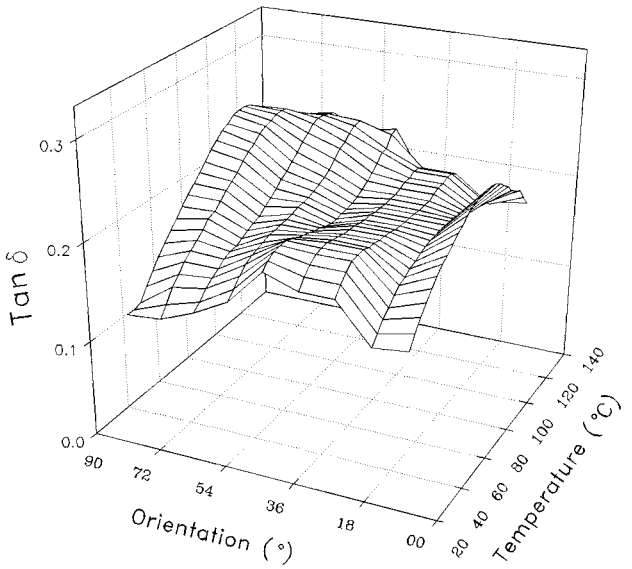

Figure 9. Tan δ surface plot for the tension-annealed film showing the orientation dependence of the mechanical α relaxation.

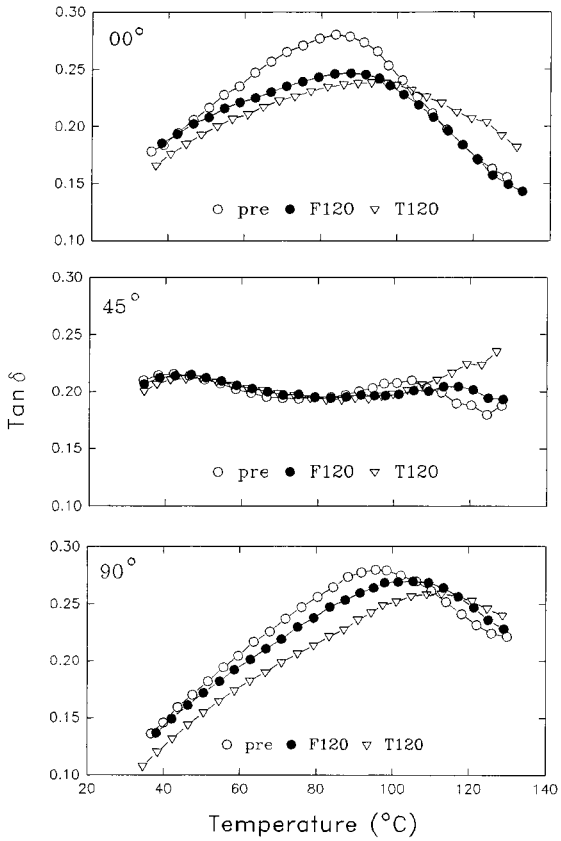

Figure 10. Tan δ for the precursor (pre), tension-annealed (T120), and free-annealed (F120) films at the 0, 45, and 90° orientations.

the three films. However, there were subtle changes for the high-temperature relaxation—this being a shift to higher temperatures for the free-annealed samples, and a disappearance of the relaxation maximum for the tension-annealed samples.

Discussion

Assignments of Mechanical α Relaxations in This Work. For the cases of the 0 and 90° oscillations, the oscillations during the dynamic mechanical tests involved the deformation of the crystalline phase and the amorphous phase as well. Due to the specific stacked lamellar texture, the HDPE film used in this

study can be considered a laminated composite composed of stacks of crystalline layers and amorphous layers. It needs to be noted that such a treatment is based on the same considerations as the two variants (parallel and series) of the Takayanagi model;[28] however, the well-defined stacked lamellar morphology of the samples provides a good justification for the above simplification. Therefore, at the 0° orientation, the two phases principally deform in series, while at the 90° orientation, they deform more in parallel. During the experiments, however, the amorphous region is in a rubbery state; therefore, the dispersion peak is not expected from the amorphous phase and must therefore come from the crystalline phase. It has been seen that the 0 and 90° oscillations were associated with activation energies of 118 or 121 kJ/mol and 185 or 195 kJ/mol (Figure 8) for the low- and high-temperature relaxations, respectively. Since these values matched well with the literature for the activation energies for the α_I and α_{II} relaxations, they are believed to be the mechanical α relaxation originating from the crystalline phase. In the above discussion, any tilt of the crystalline lamellae with respect to the MD and that of the folded polymer chains with respect to the lamellar base surface have not been taken into account.

Comparing the temperature of the relaxation peaks shown at both the 0 and 90° orientations, it was noted earlier that the 90° orientation showed a well-defined relaxation peak at a somewhat higher temperature than that of the 0° orientation. From the above discussion, it was shown that the α_I and α_{II} processes were activated in both orientations; thus, the relaxation at each orientation contained the contributions from both the α_I and α_{II} processes. Therefore, we suggest that the higher temperature α_{II} process is the dominant relaxation at the 90° orientation, whereas the lower temperature α_I process is the dominant relaxation process at the 0° orientation.

At a 45° orientation, a low activation of 88 kJ/mol was found for the low-temperature region (84 °C at 0.1 Hz), in addition to a 190 kJ/mol activation, which corresponds to the α_{II} relaxation that occurs in the high-temperature region (96 °C at 0.1 Hz). This particular orientation allows interlamellar shear to occur easily because of the maximum resolved shear stress of the applied oscillation stress on the plane of the lamellar surface. Therefore, we conjecture that interlamellar shear gives rise to the dispersion with the activation energy of 88 kJ/mol. The symmetric feature of the secondary relaxation strength with respect to the 45° orientation provided further proof for this justification, since the resolved shear stress possesses the same symmetry.[29] If the interlamellar shear indeed happened, the tie chains have to slip within the lamellae to accommodate the interlamellar shear, and this intralamellar slip could give rise to the α_{II} relaxation with an activation energy of 190 kJ/mol.

As mentioned above, while the amorphous phase is within the rubbery region, it will not generate a dispersion peak. Clearly, however, upon cooling, the vitrification of the amorphous region would be expected to introduce a mechanical relaxation. Since the interlamellar shear is basically a friction motion between crystalline lamellae and neighboring amorphous regions, the interfacial region, including the basal surfaces of the crystalline lamellae and adjacent constrained amorphous phases, is believed to be the cause of the interlamellar shear dispersion. Such a judgment has also been proposed by others based on the very long relaxation time (1−1000 s) of the mechanical α relaxation.[20]

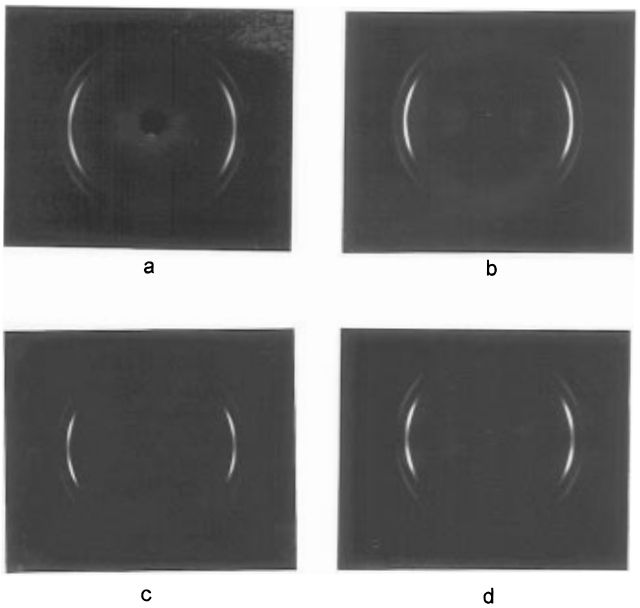

Figure 11. WAXS patterns for the precursor film before (a) and after the dynamic tests at the 0 (b), 45 (c), and 90° (d) orientations.

Effects of Morphological Changes on the Mechanical α Relaxation. As addressed earlier, it has been speculated that the morphology of the sample might change during the dynamic mechanical experiments and therefore be responsible for the observed multiplicity of the mechanical α relaxation. In order to verify if this has occurred, samples before and after the dynamic mechanical experiments were characterized by WAXS, SAXS, and DSC. In all the experiments, samples from the precursor film at the three orientations, namely 0, 45, and 90° orientations, were used. The data indeed showed that there were some morphological changes caused by the dynamic mechanical tests as will now be considered.

WAXS patterns in Figure 11 showed that the 0° oscillation has resulted in an increase in the orientation of the crystalline phase (Figure 11a,b where f_c increased from 0.67 to 0.76), whereas the 45 and 90° oscillations showed almost no effect of the dynamic mechanical tests on the orientation state of the crystalline phase relative to the precursor film (compare Figure 11c,d with Figure 11a). The increase in f_c for the sample at 0° oscillation is not surprising, since it was basically "annealed" under a dynamic tensile stress, just as the tension-annealed film, which also developed a higher value of f_c during its annealing process. It is speculated that the cause of this increase in f_c for both samples is due to the ease of translational motions of the chain axis in the crystal when a stress is applied along the original orientation axis. SAXS data (scanned along the MD) in Figure 12 also showed the morphological changes caused by the dynamic tests at the three different orientations. SAXS profiles from samples after the dynamic tests showed a more well-defined secondary scattering peak compared to the sample before the tests. In addition, the first-order scattering peak was also "sharpened" for each sample after the dynamic mechanical test. The peak positions also shifted to somewhat smaller scattering angles, indicating an increase in the long spacing for

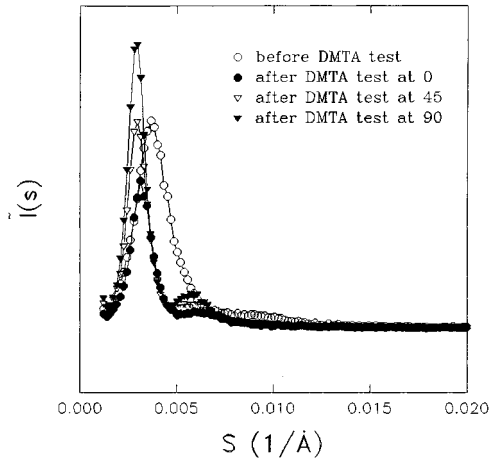

Figure 12. SAXS (MD scan) data for the precursor film before and after the dynamic tests at the 0, 45, and 90° orientations.

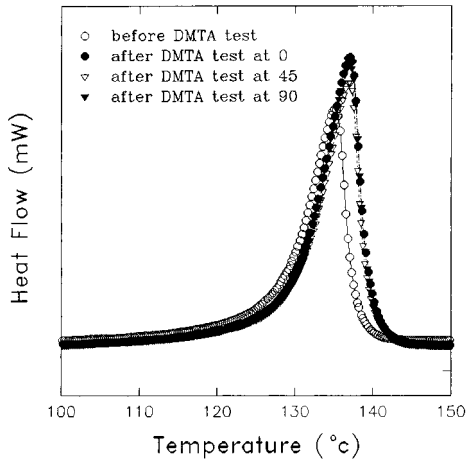

Figure 13. DSC scans for the precursor film before and after the dynamic tests at the 0, 45, and 90° orientations.

samples after the test; however, the differences between the three orientations were not major.

DSC results (Figure 13) showed that there were increases in melting point and percent crystallinity after the dynamic mechanical tests for all three orientations. The increase in melting point at all three orientations was also about the same (ca. 1.5 °C). In terms of percent crystallinity, the 0° orientation had the largest amount of increase (16%), followed by the 90° orientation (14%) and by the 45° orientation (6%); these values also implied different degrees of perfection for the crystalline lamellae after the tests. The lamellar thickness distribution curves calculated from the DSC data are presented in Figure 14. Clearly, lamellar thickness increased as a result of the dynamic mechanical tests; however, the differences among the three orientations were not significant, especially for the 0 and 90° orientations. It is realized that the calculated lamellar thickness and its distribution based on the DSC data at this heating rate may not be precise, as concluded from a detailed investigation on this issue that will be published elsewhere;[27] however, the above statement about the *relative comparison* of lamellar thickness and its distribution for samples before and after the dynamic mechanical tests is valid.

Recalling the tan δ data for precursor film obtained at the 0 and 90° orientations, which were presented in Figure 10, they show the same peak height but occur at slightly different temperatures. The peak height of the dispersion is usually related to the concentration of

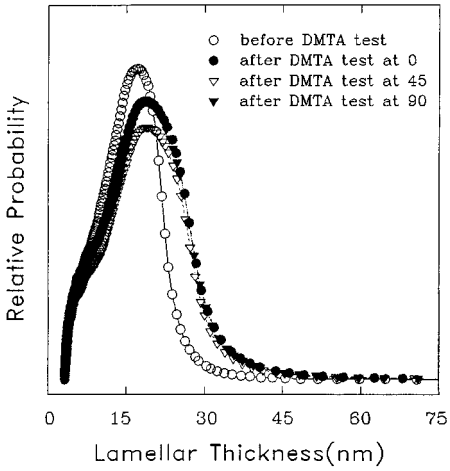

Figure 14. Lamellar thickness distributions calculated from the DSC data for the precursor film before and after the dynamic tests at the 0, 45, and 90° orientations.

mobile defects and the amount of crystalline phase, and the peak temperature has been noted to be shifted to larger values for the thicker crystalline lamellae.[30,31] From the DSC data, samples after the 0 and 90° oscillations showed basically the same change in heat of fusion (related to the amount of crystalline phase and defect concentration) and melting temperature (related to the thickness of the crystalline lamellae), and therefore the mechanical dispersion would have the same peak height and temperature as well. Although the same peak height was indeed observed in Figure 10a,c, the expected same peak temperature was not observed. Therefore, it is believed that the difference of tan δ for these two cases is not caused by the changes of morphology before and after the dynamic mechanical experiments; rather, it is mainly due to the different contributions from the α_I and α_{II} relaxations activated in the two different orientations.

For the 45° orientation, we have tentatively assigned the low-temperature relaxation to an interlamellar shear process, which is caused by the frictional nature of the shear motion. Therefore, the possible effects of the morphological changes due to the tests should be related to the changes in the interfacial region, instead of only the amount of amorphous phase in the sample. This argument is supported by the data in Figure 10b, where three films (precursor, free-annealed, and tension-annealed) with different final percent crystallinity (61, 70, and 76%) displayed the same low-temperature relaxation peak (ca. 42 °C at 0.1 Hz). We did not proceed further on this issue because of the limited knowledge at present about the crystalline lamellae/amorphous interface in this material.

It is worth pointing out that the interlamellar motion and/or dispersion have been proposed by many authors before,[7−22] but the activation energy of 88 kJ/mol has not been reported previously. Obviously, the amount of shear motion is very limited for samples having spherulitic morphology and fibril morphology as compared to the samples having a stacked lamellar morphology under the 45° oscillation; therefore, it is not possible for the interlamellar shear dispersion to stand out as a major dispersion mechanism. In addition, as discussed above, the activation energy of the interlamellar shear dispersion is dependent on the nature of the crystalline/amorphous interface, which is not commonly addressed in the literature as well; thus, it is not

surprising that the activation energies from different studies were not the same.

Molecular Origins of Mechanical α Relaxations. As pointed out earlier, the origin of the mechanical α relaxation has been extensively investigated,[1−4] and a number of molecular mechanisms have been proposed, including those that treat this relaxation as a property of the interior of the crystal and those that regard it mainly as arising from surface effects.[1−4] For the multiplicity of this relaxation, the basic assignments are (1) α_I is related to the interlamellar shear or intralamellar mosaic-block shear and (2) α_{II} is related to the interchain motion in the crystalline phase due to the anisotropy of the crystalline lattice potential. In addition, according to some authors, the multiplicity of the mechanical α relaxation is due to the distribution of crystalline lamellar thickness distribution; i. e., the different relaxation peaks correspond to the same molecular mechanism taking place in crystalline lamellae of different thickness. From our experiments, the same film showed distinctly different mechanical relaxation behavior by simply changing the direction of the dynamic oscillation with respect to the MD, regardless of the same lamellar thickness distribution at all the orientations before (same film) and after (0 and 90° orientations) the experiments. *This means that the change of tan δ cannot result only from a distribution of lamellar thickness; rather, the anisotropy of the mechanical α relaxation is also directly related to different kinds of molecular mechanisms that are excited due to the different orientation of the oscillation direction.*

In this study, the α_{II} relaxation has been found more prominent at the 90° orientation than that at the 0° orientation. That is to say the α_{II} relaxation is more clearly observed when the applied excitation is perpendicular to MD, i.e. the chain direction. These results are consistent with those obtained from the studies on the UHMwPE ultradrawn fibers, where the α_{II} relaxation strength was found to be reduced with increasing draw ratio.[17−19] Therefore, the α_{II} relaxation is believed to be due to the extreme anisotropic nature of the crystal lattice potential of the crystalline phase. In this case, incoherent lattice vibrations (crystal disordering transition) at high temperature result in greater chain motion—either rotational motion about the *c*-axis or translational motion along the *c*-axis.[32,33]

It has been shown by others that interlamellar shear indeed promotes mechanical relaxation, but it is not the α_I relaxation *per se*. It is known that interlamellar shear is the origin of the β relaxation in low-density polyethylene (LDPE),[29] and this β relaxation has even been postulated to correspond to the glass transition temperature of the amorphous portion in the LDPE.[34] Yet, for the case of HDPE, the same relaxation which might therefore correspond to the glass transition temperature of the amorphous portion in HDPE is hardly seen. Possible reasons for this are (1) the amount of amorphous phase is limited and (2) the glass transition temperature is a variable,[35] changing from the amorphous phase, which is highly constrained such that the glass transition temperature is shifted to high temperatures (so-called T_{gU}), to the unconstrained core amorphous phase, which preserves a low glass transition temperature (so-called T_{gL}). The interlamellar shear in HDPE is an interfacial frictional event; unlike the case of the β relaxation in LDPE, which corresponds to the amount of bulk amorphous phase, it is dependent upon the characteristics of the interface. It should be noted that the β relaxation has also been investigated by dynamic mechanical relaxation[36] as well as dielectric relaxation studies.[23] However, the activation energy for this β transition, which is calculated by the authors utilizing the Arrhenius equation,[23,36] was found to be *higher* than that of the α relaxation. Therefore, it is unlikely that such a β relaxation, denoted as β_a by the original authors,[23] is the same as that addressed in this study, which is believed to be induced by interlamellar shear.

Thus, we believe that the α_I process should be regarded as an intralamellar process. As proposed by Takayanagi et al.,[8−10] the intercrystal-mosaic-block shear is the origin for such a relaxation. It was further suggested by Kawai et al.[37] that the intralamellar relaxation is associated with the reorientation of crystal grains within the crystalline lamellae about the *a*- and *b*-axes. However, it should be pointed out that the existence of a mosaic-block texture within the crystalline lamellae, as originally proposed based on the SAXS studies for fibers,[38,39] has been questioned by some authors.[40,41]

Conclusion

Dynamic mechanical tests were carried out on melt-extruded uniaxially oriented HDPE films at different orientations with respect to the original MD, which displayed anisotropy of the mechanical α relaxation. In addition, the morphologies of the samples before and after the dynamic mechanical tests were also investigated. It was confirmed that the multiplicity of the mechanical α relaxation is indeed due to different molecular mechanisms rather than caused by the distribution of crystalline lamellar thickness. For the 0 and 90° orientations, the mechanical α_I and α_{II} relaxation processes were observed, whereas for the 45° orientation, an interlamellar shear related relaxation was generated as well as the mechanical α_I relaxation. The α_{II} relaxation is believed to be an intracrystalline process, and it is related to the anisotropy of the crystal lattice potential. The α_I relaxation is an intralamellar process and it is related to a grain-boundary motion within the crystalline lamellae. The interlamellar shear relaxation is related to the area and nature of the interface between crystalline lamellae and the amorphous phase.

Acknowledgment. We would like to thank Hoechst Celanese Co. for kindly providing the HDPE films.

References and Notes

(1) McCrum, N. G.; Reads, B. E.; and Willams, G. *Anelastic and Dielectric Effects in Polymer Solids*; John Wiley & Sons, New York, 1967.
(2) Boyd, R. H. *Polymer* **1985**, *26*, 1123.
(3) Boyd, R. H. *Polymer* **1985**, *26*, 323.
(4) Hoffman, J. D.; Williams, G.; Passaglia, E. *J. Polym. Sci., Part C* **1966**, *14*, 173.
(5) Stehling, F. C.; Mandelkern, L. *Macromolecules* **1970**, *3*, 242.
(6) Illers, K. H. *Kolloid Z. Z. Polym.* **1979**, *261*, 394.
(7) Nakayasu, H.; Markovitz, H.; Plazek, D. J. *Trans. Soc. Rehol.* **1961**, *5*, 261.
(8) Takayanagi, M.; Matsuo, T. *J. Macromol. Sci., Phys.* **1967**, *B1*, 407.
(9) Kajiyama, T.; Okada, T.; Sakoda, A.; Takayanagi, M. *J. Macromol. Sci.* **1973**, *B7* (3), 583.
(10) Takayanagi, M. *J. Macromol. Sci.* **1974**, *B9* (3) 391.
(11) McCrum, N. G.; Norris, E. J. *Proc. R. Soc. London, Ser. A* **1966**, *A292*, 506.
(12) Buckley, C. P.; McCrum, N. G. *J. Mater. Sci.* **1973**, *8*, 928.

(13) Yamada, R.; Stein, R. S. *J. Appl. Phys.* **1967**, *36*, 3005.
(14) Takeuchi, A.; Stein, R. S. *J. Polym. Sci., Polym. Phys. Ed.* **1967**, *5*, 1079.
(15) Stachurski, Z. H.; Ward, I. M. *J. Macromol. Sci.* **1969**, *B3*, 427.
(16) 1Stachurski, Z. H.; Ward, I. M. *J. Macromol. Sci.* **1969**, *B3*, 445.
(17) Matsuo, M.; Sawatari, C.; Ohhata, T. *Macromolecules* **1988**, *21*, 1317.
(18) Ogita, T.; Yamamoto, R.; Suzuki, N.; Mastuo, M. *Polymer* **1991**, *32*, 822.
(19) Ohta, Y.; Yasuda, H. *J. Polym. Sci., Polym. Phys. Ed.* **1994**, *32*, 2241.
(20) Alberola, N.; Cavaille, J. Y.; Perez, J. *J. Polym. Sci., Polym. Phys. Ed.* **1990**, *28*, 569.
(21) Jourdan, C.; Cavaille, J. Y.; Perez, J. *J. Polym. Sci., Polym. Phys. Ed.* **1989**, *27*, 2361.
(22) Amparo, R. G.; Ricardo, D. C. *J. Appl. Phys.* **1987**, *34*, 2819.
(23) Ashcraft, C. R.; Boyd, R. H. *J. Polym. Sci., Polym. Phys. Ed.* **1976**, *14*, 2153.
(24) Yu, Ta-hua; Wilkes, G. L. *Polymer* **1996**, *37*, 4675.
(25) Wlochowicz, A.; Eder, M. *Polymer* **1985**, *25*, 1268.
(26) Hoffman, J. D.; Miller, R. L.; Marand, H.; Roitman, D. B. *Macromolecules* **1992**, *25*, 2221.
(27) Zhou, Hongyi; Wilkes, G. L. *Polymer*, to appear.
(28) Grubb, D. T. *Materials Science and Technology: A Comprehensive Treatment*; VCH: Weinheim, New York, 1991; Vol. 12, Chapter 7.
(29) Davies, G. R.; Owen, A. J.; Ward, I. M.; Gupta, V. B. *J. Macromol. Sci. Phys.* **1972**, *B6* (1) 215.
(30) Reneker, D. H.; Mazur, J. *Polymer*, **1983**, *24*, 1387.
(31) Reneker, D. H.; Mazur, J. *Polymer*, **1982**, *23*, 401.
(32) Okano, K. *J. Polym. Sci., Part C* **1966**, *15*, 95.
(33) Peterlin, A.; Fischer, E. W. *Z. Phys.* **1961**, *159*, 272.
(34) Euns, J. B.; Simha, R. *J. Macromol. Sci., Phys.* **1977**, *B13*, 25.
(35) Boyer, R. F.; *J. Macromol. Sci., Phys.* **1973**, *B8* (3−4), 503.
(36) Boyd, R. H. *Macromolecules* **1984**, *7*, 903.
(37) Kawai, H.; Suehiro, S.; Kyu, T.; Shimomura, A. *Polym. Eng. Rev.* **1981**, *3−4*, 110.
(38) Fischer, E. W.; Lorenz, R. *Kolloid Z. Z. Polym.* **1963**, *189*, 97.
(39) Hosemann, R.; Wilke, W.; Calleja, F. J. B. *Acta Crystallogr.* **1966**, *21*, 118.
(40) Thomas, E. J.; Sass, S. L.; Kramer, E. J. *J. Polym. Sci., Polym. Phys. Ed.* **1974**, *12*, 1015.
(41) Harrison, I. R.; Keller, A.; Sadler, D. M.; Thomas, E. J. *Polymer* **1976**, *17*, 736.

MA961437N